Please cite this article in press as: Narcisi et al., Long-Term Expansion, Enhanced Chondrogenic Potential, and Suppression of Endochondral Ossification of Adult Human MSCs via..., Stem Cell Reports (2015), http://dx.doi.org/10.1016/j.stemcr.2015.01.017

Stem Cell Reports
Article

ISSCR

OPEN ACCESS

Long-Term Expansion, Enhanced Chondrogenic Potential, and Suppression of Endochondral Ossification of Adult Human MSCs via WNT Signaling Modulation

Roberto Narcisi,[1] Mairéad A. Cleary,[1,2] Pieter A.J. Brama,[2] Martin J. Hoogduijn,[3] Nesrin Tüysüz,[4] Derk ten Berge,[4,6,*] and Gerjo J.V.M. van Osch[1,5,6,*]

[1]Department of Orthopaedics, Erasmus MC, University Medical Center, 3015 CN Rotterdam, the Netherlands
[2]Section of Veterinary Clinical Sciences, School of Veterinary Medicine, University College Dublin, Belfield, Dublin 4, Ireland
[3]Department of Internal Medicine, Erasmus MC, University Medical Center, 3015 CN Rotterdam, the Netherlands
[4]Erasmus MC Stem Cell Institute, Department of Cell Biology, Erasmus MC, University Medical Center, 3015 CN Rotterdam, the Netherlands
[5]Department of Otorhinolaryngology, Erasmus MC, University Medical Center, 3015 CN Rotterdam, the Netherlands
[6]Co-senior author
*Correspondence: d.tenberge@erasmusmc.nl (D.t.B.), g.vanosch@erasmusmc.nl (G.J.V.M.v.O.)
http://dx.doi.org/10.1016/j.stemcr.2015.01.017

SUMMARY

Mesenchymal stem cells (MSCs) are a potential source of chondrogenic cells for the treatment of cartilage disorders, but loss of chondrogenic potential during in vitro expansion and the propensity of cartilage to undergo hypertrophic maturation impede their therapeutic application. Here we report that the signaling protein WNT3A, in combination with FGF2, supports long-term expansion of human bone marrow-derived MSCs. The cells retained their chondrogenic potential and other phenotypic and functional properties of multipotent MSCs, which were gradually lost in the absence of WNT3A. Moreover, we discovered that endogenous WNT signals are the main drivers of the hypertrophic maturation that follows chondrogenic differentiation. Inhibition of WNT signals during differentiation prevented calcification and maintained cartilage properties following implantation in a mouse model. By maintaining potency during expansion and preventing hypertrophic maturation following differentiation, the modulation of WNT signaling removes two major obstacles that impede the clinical application of MSCs in cartilage repair.

INTRODUCTION

Cartilage is an avascular, alymphatic, and aneural tissue (Mankin, 1982) that, consequently, has limited repair capacity. Therefore, cartilage damage requires clinical intervention. In the last two decades, cell-based therapies have emerged as promising treatment options. Autologous chondrocyte implantation (ACI) was first applied in 1994 and is still used to treat cartilage defects in human patients (Brittberg et al., 1994). In ACI, however, chondrocytes are harvested from the patient, creating an additional cartilage defect. Moreover, before use, the chondrocytes require in vitro expansion, which causes the progressive loss of cartilage matrix gene expression (Benya et al., 1978; Mayne et al., 1976).

Mesenchymal stem cells (MSCs) from adult tissues, with their ability to differentiate into several cell types, chondrocytes included, have been investigated as an alternative cell source (Dennis et al., 1999; Pittenger et al., 1999; Prockop, 1997). Unfortunately, despite their easy isolation and in vitro expansion, the loss of stem cell characteristics and differentiation potential with expansion (Banfi et al., 2000; Bonab et al., 2006; Chen et al., 2005; Li et al., 2011) and the induction of hypertrophic maturation following chondrogenic differentiation (Hellingman et al., 2010; Pelttari et al., 2006; Scotti et al., 2010) limit their appeal. Expansion of MSCs is improved in the presence of fibroblast growth factor 2 (FGF2) (Bianchi et al., 2003; Quarto et al., 2001; Solchaga et al., 2005; Tsutsumi et al., 2001), but FGF2 does not prevent the gradual loss of cell multipotency or the subsequent formation of hypertrophic cartilage (Farrell et al., 2009; Hellingman et al., 2010; Pelttari et al., 2006). A major challenge therefore is to identify the factors that support MSC expansion while maintaining their chondrogenic capacity, and additionally the factors that regulate hypertrophic maturation.

To identify such factors, we took inspiration from the process of cartilage and bone formation during embryonic development. In developing mouse limbs, skeletal tissues are generated by a rapidly expanding population of multipotent mesenchymal cells, found at the tip of the embryonic limb bud (Rabinowitz and Vokes, 2012; Zeller et al., 2009). The expansion of these multipotent cells is driven by the combination of WNT and FGF signals, secreted by the apical ectodermal ridge (ten Berge et al., 2008a). The combination of WNT and FGF proteins synergistically supports the expansion of these cells in vitro while maintaining their multilineage potential (Cooper et al., 2011; ten Berge et al., 2008a). Furthermore, WNT signals also play an important role during cell differentiation, where their ability to modulate chondrogenesis and induce osteogenesis is well established both in vitro (Churchman et al., 2012;

Please cite this article in press as: Narcisi et al., Long-Term Expansion, Enhanced Chondrogenic Potential, and Suppression of Endochondral Ossification of Adult Human MSCs via..., Stem Cell Reports (2015), http://dx.doi.org/10.1016/j.stemcr.2015.01.017

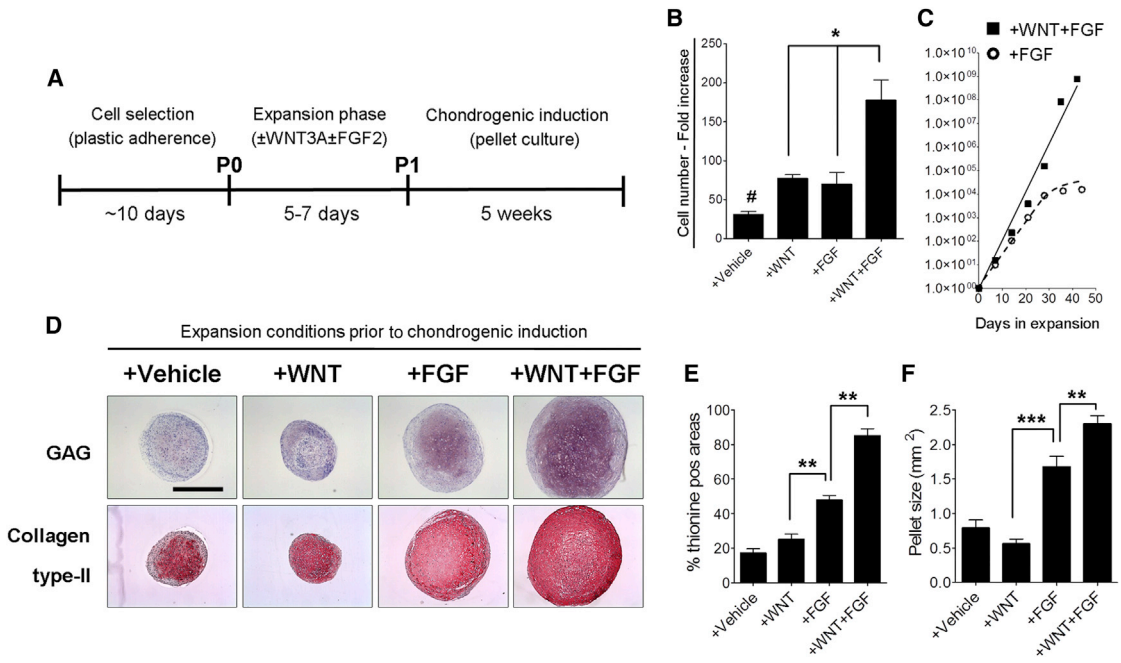

Figure 1. WNT3A in Combination with FGF2 Enhances Expansion and Chondrogenic Potential of MSCs

(A) Schematic overview of the experimental protocol. P0, passage 0; P1, passage 1.

(B and C) Proliferation rate of MSCs after 10 days of expansion (B; n = 4 donors) or up to six passages (C; n = 1 donor) (each symbol represents a passage) in the indicated media. Lines indicate the polynomial regression representatives of the number of WF-MSCs (+WNT+FGF; solid) or F-MSCs (+FGF; dotted).

(D) Thionine staining (glycosaminoglycan; GAG) and collagen type II immunostaining of representative sections from cartilage pellets formed with cells expanded in the indicated conditions (n = 3 donors with three pellets per donor) after 5 weeks of chondrogenic induction. The scale bar represents 1 mm.

(E) Analysis of the thionine-positive areas of pellet cultures chondrogenically differentiated in the indicated conditions (n = 3 donors with three pellets per donor).

(F) Analysis of the pellet size of differentially expanded MSCs (n = 3 donors with three pellets per donor).

Values represent means ± SEM of three donors. *p < 0.05, **p < 0.01, ***p < 0.001, #p < 0.01 compared to the other conditions.

Dong et al., 2007; Jullien et al., 2012) and in vivo (Day et al., 2005; Quarto et al., 2010a, 2010b).

In this paper, we show that the combination of WNT3A and FGF2 supports extensive expansion of adult human bone marrow-derived MSCs over multiple passages while maintaining robust chondrogenic potential. Furthermore, we show that inhibition of WNT signals during chondrogenic differentiation prevents undesired hypertrophic maturation, allowing the formation of stable cartilage in vivo.

RESULTS

WNT3A and FGF2 Synergistically Promote MSC Proliferation and Chondrogenic Potential

MSCs were isolated from adult human bone marrow aspirates by selective plastic adherence (Figure 1A), followed by phenotypic characterization using flow cytometry. This confirmed the cells were positive (>95%) for the MSC markers CD73, CD90, and CD105 and negative (<0.5%) for the hematopoietic marker CD45 (Figure S1A). Afterward, we verified that MSCs responded to WNT3A protein by demonstrating the accumulation of nonphosphorylated β-CATENIN (Figure S1B) and induction of the WNT target gene *AXIN2* (Figure S1C). Treatment with FGF2 did not influence nonphosphorylated β-CATENIN accumulation (Figure S1B).

We next analyzed the effects of WNT3A and FGF2 on cell proliferation. We observed that treatment of MSCs with either WNT3A or FGF2 enhanced cell proliferation to a similar degree (Figure 1B). Moreover, proliferation was further increased by combining WNT3A with FGF2, showing a synergistic effect of the two factors (Figure 1B; fold increase in cell number compared to +vehicle: +WNT = 1.53; +FGF = 1.29; +WNT+FGF = 4.81). The synergistic action of WNT3A and FGF2 maintained a constant exponential expansion even after six passages, leading to

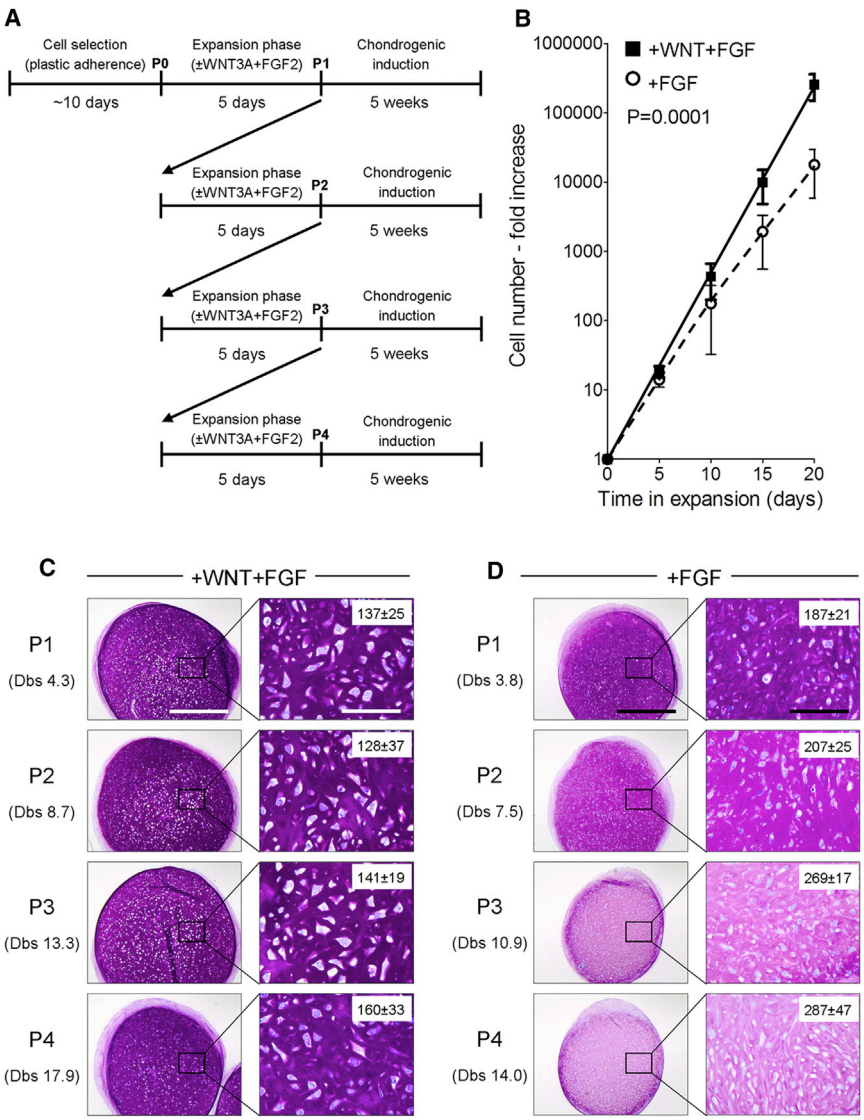

Figure 2. WNT3A in Combination with FGF2 Maintains Robust Chondrogenic Potential of MSCs over Multiple Passages

(A) Schematic of the experimental plan.

(B) Cell-number analysis during MSC expansion. Lines indicate the polynomial regression representatives of the number of WF-MSCs (+WNT+FGF; solid) or F-MSCs (+FGF; dotted). Values represent means ± SEM (n = 3 donors, three to four pellets per donor).

(C and D) MSCs were expanded for up to four passages in the indicated conditions, and pellet cultures were initiated after each passage (n = 3–5 MSC donors each passage, three pellets per donor). Shown are representative sections of the pellets after 5 weeks of chondrogenic induction, stained for glycosaminoglycans (thionine staining). Right: higher magnification of the inset areas. Numbers of cells per mm^2 are indicated in the right panels (values represent the mean ± SEM of measurements performed in three different pellets from three MSC donors). The scale bars represent 1 mm (left panels) and 200 μm (right panels). Dbs, cell doublings.

an approximately 10^9-fold expansion, whereas in the presence of FGF alone expansion slowed down over time and came practically to a halt after 30 days (Figure 1C).

Upon differentiation in pellet culture, although the chondrogenic differentiation of MSCs was performed using the same chondrogenic medium composition, MSCs expanded in the presence of both WNT3A and FGF2 (WF-MSCs) displayed an increased chondrogenic capacity compared to cells expanded in the presence of FGF2 alone (F-MSCs) (Figures 1D and 1E). Interestingly, WF-MSCs formed larger pellets (Figure 1F) that contained higher levels of the cartilage matrix components collagen type II and glycosaminoglycans (Figures 1D and 1E). Nonetheless, total cell numbers in the pellets were comparable throughout the chondrogenic induction and between the conditions, indicating that WF-MSCs produced more cartilage matrix per cell upon differentiation compared to F-MSCs (Figure S2). Cells expanded in the absence of FGF2, regardless of the presence of WNT3A, displayed a limited chondrogenic differentiation capacity (Figure 1D). Together, these data indicate that WNT and FGF synergize to not only increase proliferation but also enhance the chondrogenic potential of MSCs after short-term expansion.

We next asked whether WF-MSCs could maintain their chondrogenic potential when expanded over multiple passages. We passaged the cells every 5 days and assessed their chondrogenic potential by pellet culture at every passage (Figure 2A). Although WF-MSCs expanded faster (Figure 2B), they maintained robust chondrogenic potential over the course of four passages (Figure 2C), whereas F-MSCs gradually lost their ability to produce an extracellular matrix rich in glycosaminoglycans (Figure 2D).

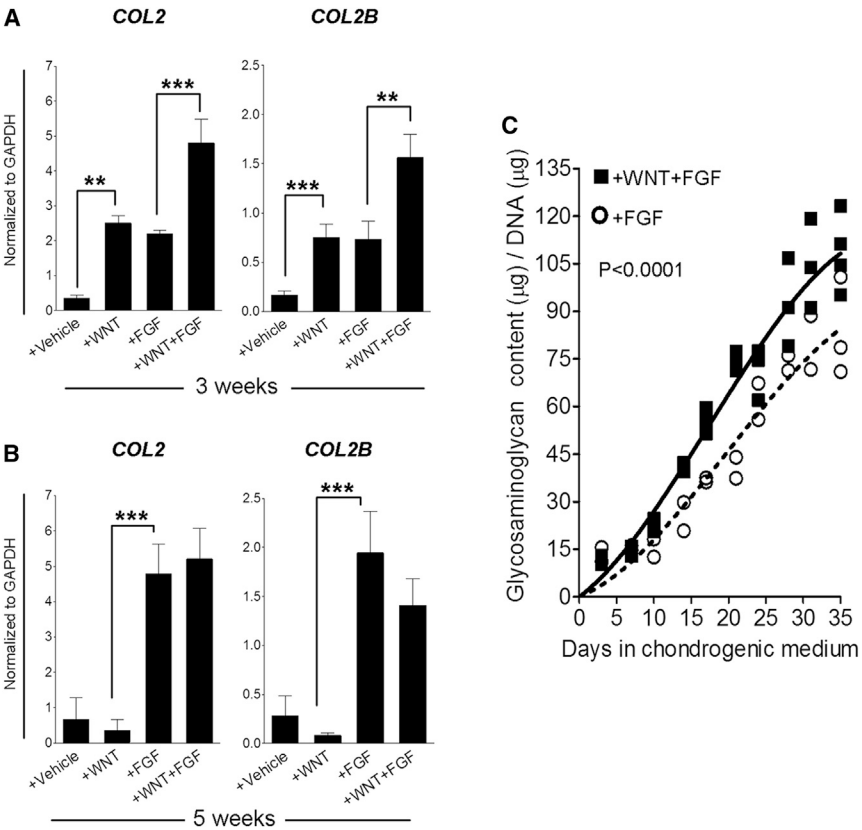

Figure 3. MSCs Expanded in the Presence of WNT3A and FGF2 Display Accelerated Chondrogenesis

(A and B) Relative gene expression levels of *COL2* and *COL2B* in pellet cultures from cells expanded in the indicated conditions after 3 (A) or 5 (B) weeks of chondrogenic induction. Values represent means ± SEM (n = 3 donors with three pellets per donor). **p < 0.01, ***p < 0.001.

(C) Relative glycosaminoglycan content of pellet cultures from cells expanded in the indicated conditions. Lines indicate the polynomial regression representatives of the glycosaminoglycan accumulation in the WF-MSCs (+WNT+FGF; solid) and F-MSCs (+FGF; dotted).

Cell-count analysis showed that pellets derived from WF-MSCs contained more extracellular matrix and lower cell density than pellets from F-MSCs (Figures 2C and 2D, right panels). These observations demonstrate that both WNT and FGF signals are required for the long-term expansion of MSCs with high chondrogenic potential.

An additional benefit of the presence of WNT3A and FGF2 during MSC expansion appeared when we observed the faster differentiation of WF-MSCs compared to F-MSCs: 3 weeks after chondrogenic induction, expression levels of collagen type II (*COL2*) and collagen type IIB (*COL2B*; a splice variant of collagen type II expressed during late chondrogenesis; McAlinden et al., 2008) were twice as high in WF-MSCs as in F-MSCs (Figure 3A). After 5 weeks, at the end of the differentiation protocol, transcript levels were not significantly different from each other (Figure 3B; +FGF versus +WNT+FGF), indicating that the increased collagen type II protein accumulation we observed (Figure 1D) was the result of increased deposition earlier during differentiation. In agreement with this, we observed that glycosaminoglycans accumulated faster in pellets formed with WF-MSCs than in F-MSC pellets (Figure 3C).

Although MSCs can express several WNT ligands (Cho et al., 2006; Etheridge et al., 2004), endogenous WNT signaling appears to play a negligible role in MSC expansion, because we found no effects on cell proliferation or subsequent differentiation when endogenous WNT proteins were blocked by the WNT antagonist Fz8CRD or when endogenous WNT production was inhibited by the porcupine inhibitor IWP2 (Figure S3).

Together, these results demonstrate that WNT3A, in cooperation with FGF2, not only enhances long-term MSC chondrogenic potential but also accelerates their subsequent chondrogenic differentiation.

In Vitro WNT Signaling Modulation Leads to Stable Cartilage Formation In Vivo

A major obstacle preventing the use of MSCs for cartilage repair is their tendency to initiate endochondral ossification following chondrogenic differentiation. This can be observed as accumulation of collagen type X (*COL10*), matrix metalloproteinase 13 (*MMP13*; also known as collagenase 3), and alkaline phosphatase (*ALP*) during hypertrophic maturation (Hellingman et al., 2010, 2011), followed by calcification of the tissue and blood vessel invasion, steps that ultimately lead to bone formation (Farrell et al., 2011; Scotti et al., 2010). Encouragingly, although WF-MSCs demonstrated an enhanced chondrogenic potential, they did not display an increase in collagen type X protein accumulation during chondrogenic differentiation

(Figure 4A). Although *COL10* expression was upregulated after 3 weeks in pellet culture, in line with the faster *COL2* production, it did not further increase during the last 2 weeks of differentiation (Figure 4B). In contrast, F-MSCs continued to increase *COL10*, ultimately resulting in higher expression after 5 weeks of differentiation (Figure 4B). Moreover, WF-MSCs also expressed lower levels of *MMP13* at both time points (Figure 4C). This suggests that WF-MSCs may have a lower propensity to undergo hypertrophic maturation during chondrogenic induction.

We further investigated the stability of the cartilage by implanting the differentiated pellets subcutaneously in immunocompromised (NMRI nu/nu) mice for 8 weeks (Figure 4D), a well-established model for testing cartilage stability in vivo (De Bari et al., 2004; Pelttari et al., 2006). We found that F-MSC-derived pellets displayed weak collagen type II staining, large areas of calcification, and blood vessel invasion (Figure 4E, left panels), indicating the onset of endochondral ossification. In contrast, WF-MSC-derived pellets were strongly positive for collagen type II and displayed no blood vessel invasion after implantation (Figure 4E, right panels). However, calcified cartilage was observed, indicating that WF-MSCs ultimately underwent endochondral ossification in vivo, although the process may be delayed (Figure 4E).

Multiple reports indicate that WNT signals promote osteogenic differentiation of multipotent progenitors during endochondral ossification (Cawthorn et al., 2012; Day and Yang, 2008). Indeed, the WNT target *AXIN2* was expressed in MSCs during chondrogenic differentiation and repressed by IWP2, indicating it was due to endogenous WNT signals (Figure 4F). We therefore tested whether inhibition of WNT signals during chondrogenic induction would prevent hypertrophic maturation. When chondrogenic differentiation was performed in the presence of IWP2, both F-MSCs and WF-MSCs showed reduced *AXIN2* expression (Figure 4F). Although only small changes in *COL10* and *MMP13* mRNA levels were observed, *ALP* was strongly downregulated by IWP2 (Figure 4F). Interestingly, WF-MSC-derived pellets displayed the lowest levels of *AXIN2*, *COL10*, *MMP13*, and *ALP* and the highest levels of glycosaminoglycan deposition and *COL2*, resulting in the greater *COL2*:*COL10* ratio, particularly in the presence of IWP2 (Figures 4F and 4G, upper panels; Figure S4). Importantly, upon implantation in NMRI nu/nu mice, the IWP2-treated pellets derived from WF-MSCs displayed strong collagen type II staining, with no signs of calcification or blood vessel invasion (Figure 4G). Altogether, these results show that inhibition of endogenous WNT production interferes with hypertrophic maturation and supports the formation of cartilage from WF-MSCs that remains stable in our in vivo model.

WNT3A and FGF2 Maintain MSC Phenotype, Gene Expression, and Multipotency over Multiple Passages

Because MSCs from bone marrow constitute a heterogeneous population of cells (Muraglia et al., 2000; Pittenger et al., 1999), our findings suggest that, in the absence of WNT signals, the chondrogenic progenitors are gradually depleted during expansion. In order to evaluate this hypothesis, we characterized the cells prior to chondrogenic differentiation. Whereas WF-MSCs maintained a polygonal-like phenotype during expansion, F-MSCs gradually acquired a more heterogeneous and enlarged morphology (Figure 5A; Figure S5A). We further characterized the phenotypic composition of the expanding population using flow cytometry for the MSC markers CD90, CD105, CD73, CD166, CD271, and CD146 (Dominici et al., 2006; Hermida-Gómez et al., 2011; Sacchetti et al., 2007). At passage 1, >90% of the cells expressed the MSC markers CD90, CD105, CD73, and CD166 regardless of the presence of WNT3A (Figure 5B). Moreover, WF-MSCs displayed a higher expression of CD271, a protein associated with the chondrogenic subset of MSCs (Figure 5B) (Hermida-Gómez et al., 2011). CD146, which in bone marrow may be a marker of osteoprogenitor (Sacchetti et al., 2007), was lost from the cells independent of treatment with WNT3A (Figure S5B).

Following expansion over four passages, F-MSCs had decreased expression of CD90 and CD105, whereas this expression was maintained in the presence of WNT3A (Figure 5B). Furthermore, CD73 decreased in the absence of WNT3A, whereas CD166 decreased in both conditions but less in the presence of WNT3A (Figure 5B). Combined, these data suggest that WNT3A in combination with FGF2 preferentially allowed the expansion of MSCs characterized by polygonal morphology, small cell size, and high expression of CD90, CD105, CD73, CD166, and CD271. Moreover, we investigated whether multipotency of the cells was maintained (Figure 5C), and found that WNT3A in combination with FGF2 retained the adipogenic and osteogenic potential of the cells, even after four passages (Figures 5D and 5E).

Finally, we investigated how WNT and FGF affect the expression of genes involved in proliferation and cell-fate commitment. *MYC* genes mediate the proliferative effect of WNT in mouse chondrogenic progenitors (ten Berge et al., 2008a). Interestingly, WNT3A and FGF together maintained high levels of *MYC* and *NMYC*, although their expression declined in the absence of WNT3A (Figure 5F). The third *MYC* family member, *MYCL1*, was not detected (data not shown). *TWIST1* is associated with the uncommitted and proliferative state of MSCs (Isenmann et al., 2009) by stimulating *ID1* and influencing cell differentiation via the regulation of lineage-specific transcription factors (Menicanin et al., 2010; Yang et al., 2011). Again, WNT3A together with FGF2 maintained high levels of

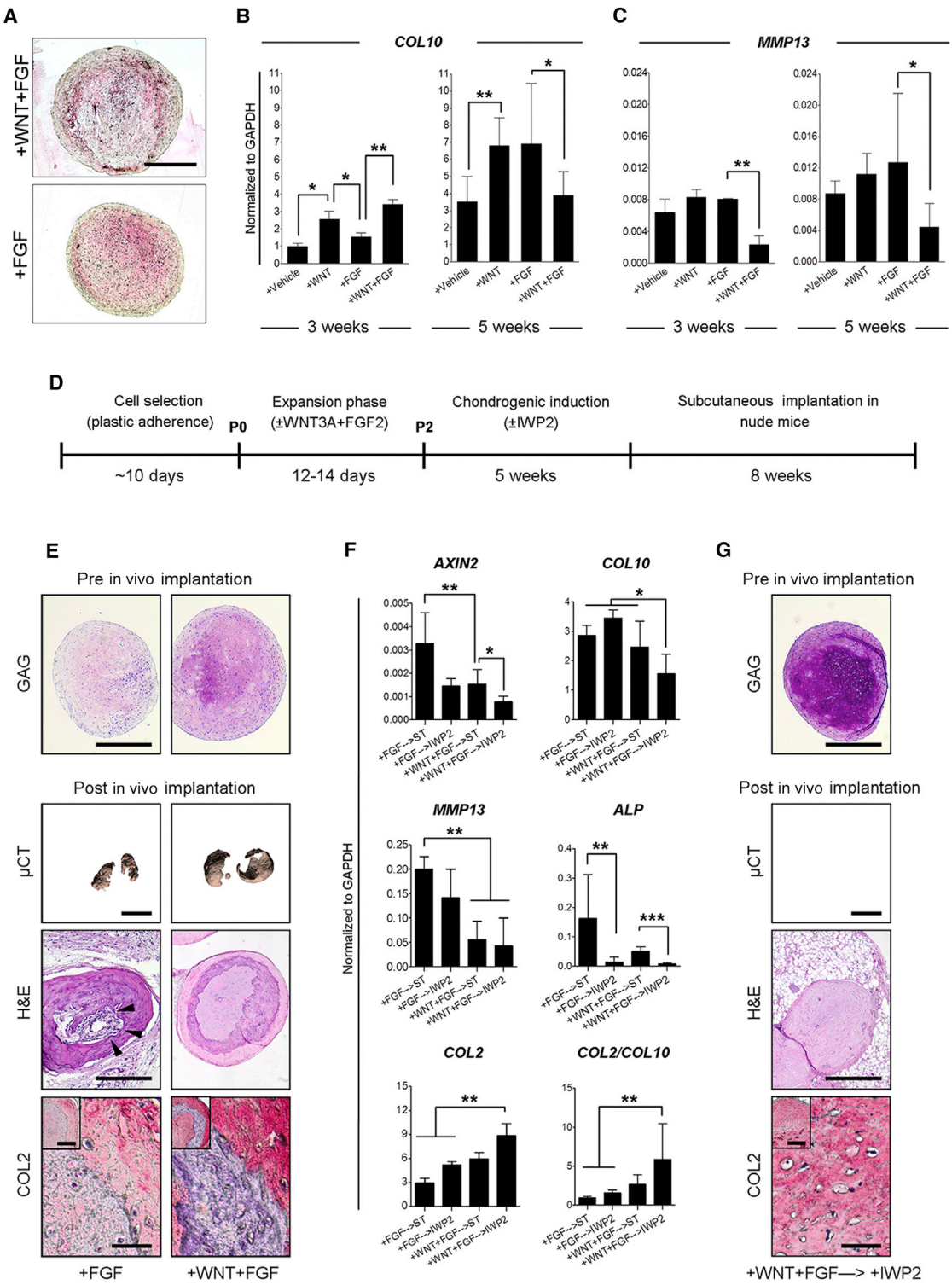

Figure 4. WNT Signaling Modulation In Vitro Prevents the Onset of Endochondral Ossification In Vivo

(A) Collagen type X immunostaining on pellet cultures obtained from WF-MSCs (+WNT+FGF) or F-MSCs (+FGF). Representative images of three MSC donors. The scale bar represents 1 mm.

(legend continued on next page)

TWIST1, *ID1*, and the chondrogenic master regulator *SOX9*, whereas the levels of these markers declined with the expansion in the absence of WNT3A (Figure 5F). Interestingly, *TWIST1*, *ID1*, and *SOX9* were not responsive to either WNT3A or FGF2 but only responded to simultaneous stimulation of these factors (Figure S5C), suggesting a possible mechanism for their synergistic effect. Combined, these data suggest that the combination of WNT3A and FGF2 maintains the uncommitted and proliferative state of MSCs by supporting the expression of *TWIST1* and *MYC* genes while maintaining their chondrogenic potential by supporting *SOX9* expression.

DISCUSSION

MSCs from adult tissues are currently used in cartilage tissue engineering but gradually lose their stem cell characteristics during in vitro expansion, leading to a decreased chondrogenic differentiation capacity (Banfi et al., 2000; Bonab et al., 2006; Chen et al., 2005; Li et al., 2011). Moreover, the cartilage undergoes hypertrophic maturation (Farrell et al., 2011; Hellingman et al., 2011). In this study, we demonstrate that MSCs from adult human bone marrow depend on WNT signals to maintain their chondrogenic potential during expansion. Furthermore, by inhibiting WNT signaling during the subsequent chondrogenic differentiation phase, we not only enhanced chondrogenesis further but also prevented the onset of endochondral ossification in our in vivo model (Figure 6). Several additional benefits arose from the use of WNT3A protein during expansion of MSCs: the cells proliferated faster, their subsequent chondrogenic differentiation took less time, and expression of hypertrophic markers was reduced. These findings have the potential to remove several major obstacles to clinical application of MSCs in the repair of large cartilage defects, reducing the time of culture while increasing the quality of the engineered cartilage and preventing calcification.

The positive effect of FGF2 on enhancing proliferation and chondrogenic potential of MSCs is well established (Handorf and Li, 2011; Mastrogiacomo et al., 2001; Solchaga et al., 2005; Tsutsumi et al., 2001). Whereas we find that FGF2 sustains cell proliferation for up to ~20 cell doublings, some reports show that it sustains cell proliferation up to 40–50 cell doublings (Auletta et al., 2011; Banfi et al., 2000; Gharibi and Hughes, 2012; Solchaga et al., 2010). However, in these studies, healthy and young donors (an average of 30 years old) were used, whereas we investigated cells from elderly patients, who are more likely to require cartilage repair. In addition, these studies report an average of 22 doublings in 40 days, whereas we find that WNT3A and FGF2 support 30 cell doublings in this time frame, despite the increased age of the donors. Thus, WNT3A not only sustains prolonged FGF2-promoted cell expansion but also enhances the proliferation rate.

MSCs can express several WNT ligands (Cho et al., 2006; Etheridge et al., 2004). This endogenous WNT signaling may play a negligible role in MSC expansion, because we found no significant effects on cell proliferation or subsequent differentiation when endogenous WNT proteins were prevented. However, and in agreement with our findings, it has been reported that inhibition of endogenous WNT signaling specifically during MSC differentiation increased their chondrogenic differentiation (Im et al., 2011; Im and Quan, 2010). Furthermore, a decreased level of β-CATENIN in differentiating MSCs was previously associated with the downregulation of the hypertrophic marker *COL10* (Venkatesan et al., 2012), consistent with our finding that WNT repression suppressed the induction of hypertrophic markers.

We show that adult human MSCs expanded with WNT3A and FGF2 retained some of their surface markers after extensive expansion in vitro. WNT3A and FGF2 may specifically support the expansion of a chondrogenic or multipotent subset of MSCs, preventing the gradual accumulation of cells that do not contribute to chondrogenesis.

(B and C) Gene expression analysis of the hypertrophic markers *COL10* (B) and *MMP13* (C) on pellet cultures after 3 or 5 weeks of chondrogenic induction. Pellets were obtained from MSCs (n = 3 donors and three pellets per donor) expanded in the indicated conditions. Values represent means ± SEM. *$p < 0.05$, **$p < 0.01$.

(D) Schematic overview of the in vivo experimental protocol.

(E) Pre and post in vivo analysis of pellets formed using F-MSCs (+FGF) or WF-MSCs (+WNT+FGF). GAG: thionine staining. The scale bar represents 1 mm. μCT: Quantum FX μCT 3D images of the calcified area of two representative pellets per condition. The scale bar represents 2 mm. H&E: hematoxylin and eosin staining on histological sections of decalcified samples. Black arrowheads indicate blood vessel invasion. The scale bar represents 1 mm. COL2: collagen type II immunohistochemistry on pellet cultures. The scale bars represent 150 μm (high magnification) and 400 μm (low magnification).

(F) Transcript analysis of pellet cultures formed with cells expanded in the indicated conditions and chondrogenically induced without (→ST) or with IWP2 (→IWP2). Values represent means ± SEM of three pellets from three MSC donors. *$p < 0.05$, **$p < 0.01$, ***$p < 0.001$.

(G) Pre and post in vivo analysis of pellets formed using WF-MSCs chondrogenically differentiated with IWP2 (+WNT+FGF→IWP2). The in vivo data are representative of samples from two MSC donors, four pellets per donor and condition. Scale bars are as defined in (E).

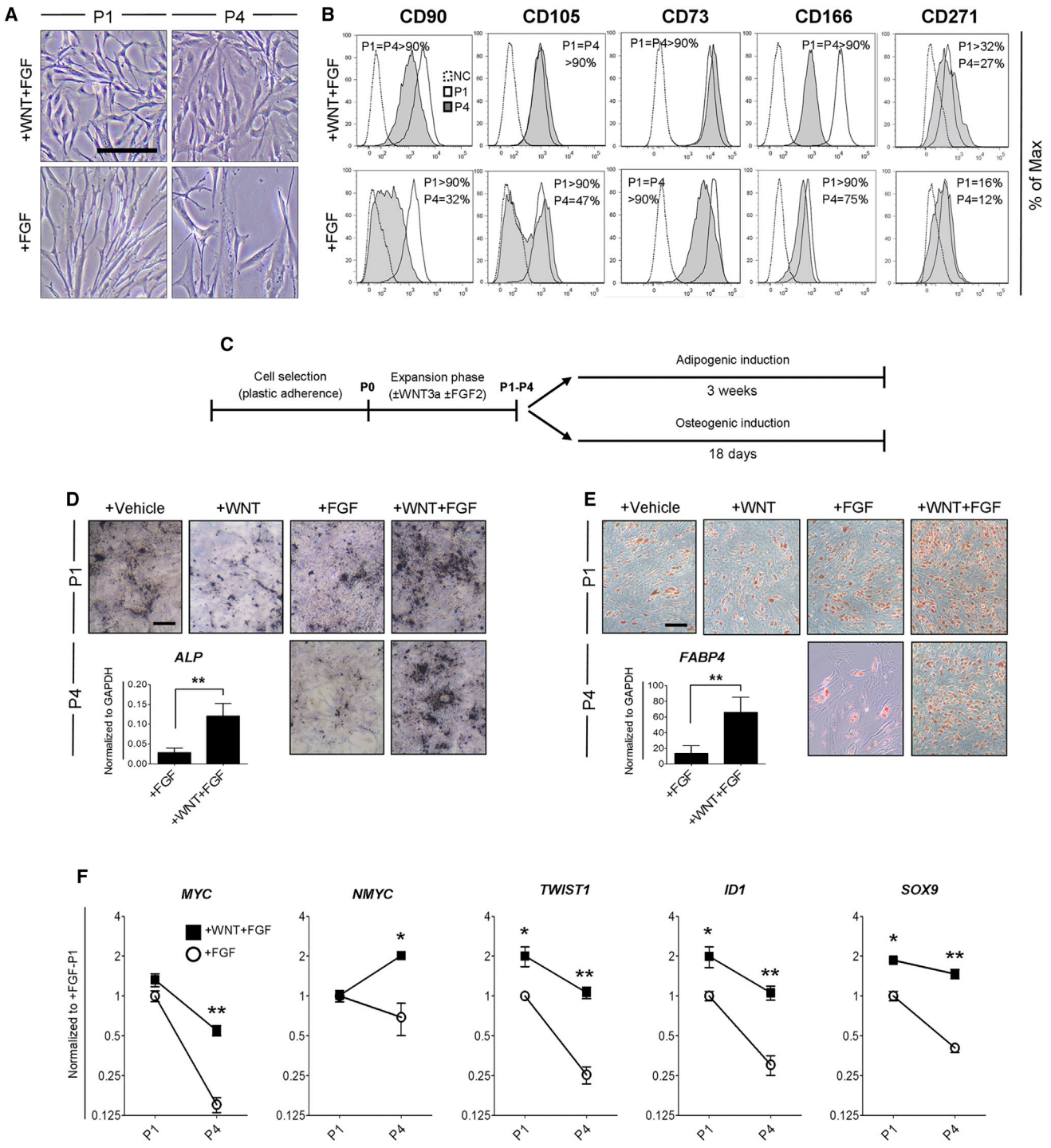

Figure 5. WNT3A and FGF2 Maintain MSC Characteristics in Multiple Passages

(A) Cell morphology of MSCs expanded as indicated. The scale bar represents 200 μm.

(B) Flow cytometry analysis of WF-MSCs (+WNT+FGF) and F-MSCs (+FGF). The percentage represents the number of positive cells for the indicated surface marker. Values are the mean of two MSC donors. NC, negative control.

(C) Schematic representation of the working plan for the multilineage differentiation.

(D) Von Kossa staining (calcium phosphate deposits) and *ALP* mRNA levels of MSCs expanded in the indicated conditions and subsequently differentiated in osteogenic medium. The scale bar represents 150 μm.

(legend continued on next page)

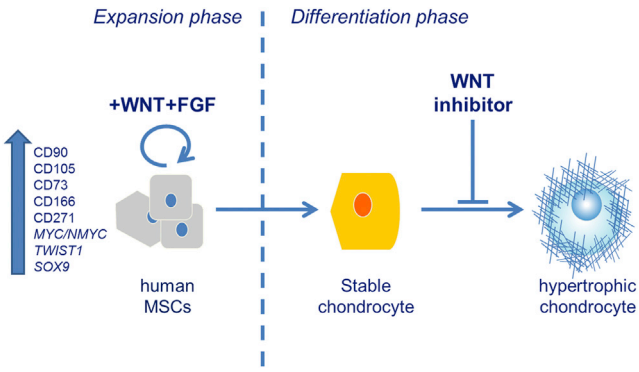

Figure 6. WNT Signaling Modulation Regulates Cell Fate of MSCs
WNT and FGF proteins maintain human MSCs in a multipotent and proliferative state. Blocking WNT signaling during chondrogenic differentiation prevents hypertrophic maturation of the cells.

Evidence for this is the loss of *SOX9* expression and the accumulation of CD90-, CD105-, CD166-, and CD271-negative populations in the absence of WNT3A. Selective maintenance of a chondrogenic subpopulation may also explain the accelerated chondrogenesis that WF-MSCs undergo. CD146 was identified as a marker for bone marrow-derived MSCs with osteoprogenitor capacity in vivo (Sacchetti et al., 2007). Upon expansion with FGF2, with or without WNT3A, we find no CD146 expression; however, the cells retain proliferation and multilineage differentiation potential, in particular in the presence of WNT3A. Thus, although CD146 may be an in vivo marker for MSCs, it does not mark multipotent MSCs after in vitro expansion.

Genes associated with the WNT pathway have been indicated as potential candidates to maintain MSCs in an uncommitted state and to enhance their proliferation capacity (Boland et al., 2004; Cho et al., 2006). We have previously shown that WNT and FGF signals interact during embryonic cartilage development to stimulate mesenchymal cell proliferation while maintaining their multipotency (ten Berge et al., 2008a). In that system, WNT and FGF synergize in promoting cell proliferation by inducing *NMYC*, which mediates cell-cycle entry in response to proliferative signals while simultaneously preventing chondrogenic differentiation by repressing the essential chondrogenic regulator *SOX9* (ten Berge et al., 2008a). This difference may arise from the different experimental contexts: whereas our human MSCs were in an undifferentiated, expanding state, the mouse cells had started to differentiate along the chondrogenic lineage, thereby strongly upregulating *SOX9*. Whereas in the mouse system, WNT prevents the upregulation of *SOX9*, in expanding human MSCs the maintenance of *SOX9* may indicate the preservation of chondrogenic potential. Consistent with this, the induction of *SOX9* goes in parallel with a synergistic effect of WNT3A and FGF2 on *TWIST1* expression, a marker commonly associated with an uncommitted state (Isenmann et al., 2009; Menicanin et al., 2010).

Our findings underline the importance of stage-dependent modulation of WNT signals in leading MSCs toward a stable cartilage fate, and also indicate how insights obtained from developmental biology contribute to generating new strategies for regenerative medicine. Prior to clinical translation, more prolonged in vivo experiments in larger animals may be needed to validate the benefit of WNT signaling modulation. Moreover, alternative delivery methods for the cells, for example cell suspensions in injectable hydrogels, may increase the applicability for tissue-engineering approaches.

EXPERIMENTAL PROCEDURES

Purified WNT3A and WNT Inhibitors

WNT3A was purified from cell-culture medium conditioned by *Drosophila* S2 cells modified with a mouse WNT3A expression vector as described (Willert et al., 2003). The purified protein was obtained as a solution of 50 μg ml^{-1} in PBS + 1% 3-[(3-cholamidopropyl)dimethylammonio]-1-propanesulfonate (CHAPS). The competitor of the WNT receptor Frizzled, Fz8CRD, was produced as a fusion protein (Fz8CRD-IgG) as previously described (Hsieh et al., 1999). The WNT-secretion inhibitor *N*-(6-methyl-2-benzothiazolyl)-2-[(3,4,6,7-tetrahydro-4-oxo-3-phenylthieno[3,2-d]pyrimidin-2-yl)thio]-acetamide (IWP2) was purchased from Stemgent and dissolved in DMSO, obtaining a stock solution of 2 mM. IWP2 specifically inhibits the maturation (endogenous production) of WNT proteins by blocking the acyltransferase enzyme porcupine.

Cell Source and Isolation of MSCs from Bone Marrow

Adult human MSCs from bone marrow were obtained from femoral biopsies of donors (age 50–78 years) undergoing total hip replacement, after signed informed consent and with approval of the local ethical committees (Erasmus MC number MEC-2004-142; Albert Schweizer Hospital number 2011.07). Cells from bone marrow aspirates were seeded at a density of approximately

(E) Oil red O staining (lipid accumulation) and *FABP4* mRNA levels of MSCs expanded in the indicated conditions and subsequently differentiated in adipogenic medium. The scale bar represents 100 μm.
Transcript analysis in (D) and (E) was performed on P4 expanded cells. Images of P1 cells are representative of two independent MSC donors; P4 images are representative of three MSC donors. $^{**}p < 0.01$.
(F) Gene expression profile of MSCs expanded in the indicated conditions prior to differentiation. Values represent means ± SEM. The data are representative of three MSC donors with two biological replicates per donor. $^{*}p < 0.05$, $^{**}p < 0.01$.

50,000 nucleated cells cm^{-2} in alpha-MEM (GIBCO), supplemented with 10% fetal calf serum (FCS), 1 ng ml^{-1} FGF2 (AbD Serotec), 25 μg ml^{-1} ascorbic acid-2-phosphate (Sigma-Aldrich), 1.5 μg ml^{-1} fungizone, and 50 μg ml^{-1} gentamicin. MSCs were isolated by their ability to adhere to plastic culture flasks. After 24 hr, nonadherent cells were washed out and adherent cells were cultured in standard conditions (5% CO_2 at 37°C) for 10 ± 2 (mean ± SD, n = 6 donors) days. Medium was renewed three times per week. When MSCs neared confluence, they were detached with 0.05% trypsin and characterized by flow cytometry. Cells were resuspended at 750,000 cells ml^{-1} in FACSFlow solution (BD Biosciences).

Expansion Phase

After isolation, MSCs were trypsinized using 0.05% trypsin and reseeded at a density of 2,300 cells cm^{-2} in alpha-MEM + 10% FCS + 25 μg ml^{-1} ascorbic acid-2-phosphate supplemented as follows:

(1) no supplementation (+vehicle)
(2) + 250 ng ml^{-1} WNT3A (+WNT)
(3) + 1 ng ml^{-1} FGF2 (+FGF)
(4) + 250 ng ml^{-1} WNT3A + 1 ng ml^{-1} FGF2 (+WNT+FGF)
(5) + 250 ng ml^{-1} WNT3A + 1 ng ml^{-1} FGF2 + 2 μM IWP2 (+WNT+FGF+IW)
(6) + 1 ng ml^{-1} FGF2 + 2 μM IWP2 (+FGF+IW)
(7) + 1 ng ml^{-1} FGF2 + 2 μg ml^{-1} Fz8CRD (+FGF+FZ).

The concentrations of WNT3A and FGF2 used were based on previous reports (Martin et al., 1997; ten Berge et al., 2008b, 2011). Vehicle consisted of PBS + 1% CHAPS and/or DMSO, as applicable. Medium was renewed every 24 hr. After one passage (P1), cells were harvested, counted, and used to assay the chondrogenic potential by pellet culture. Alternatively, MSCs were expanded up to P4 using an expansion condition in the presence of FGF2 or WNT3A and FGF2. With every passage in a monolayer, cells were harvested, counted, and then transferred to a pellet-culture system to assess the chondrogenic potential or replaced for the next expansion. Cell doublings were determined using the following formula: doublings = $\log_2$ (cells at the end of the passage/cells seeded).

FACS Analysis

Cells were resuspended at 750,000 cells ml^{-1} in FACSFlow solution (BD Biosciences) and stained with antibodies against human CD45-PerCp (345809), CD73-PE (550257), CD140a-PE (556002), CD146-FITC (560846), CD166-PE (559263), CD271-Alexa Fluor (560326) (BD Biosciences), CD90-APC (FAB2067A), and CD105-FITC (FAB10971F) (R&D Systems), following the manufacturer's guidelines. Unstained samples were used as negative controls. Flow cytometry analysis was performed using the BD FACSCanto II apparatus (BD Biosciences), and data were analyzed using BD FACSDiva software (BD Biosciences).

Chondrogenic Differentiation

After expansion, MSCs were harvested and centrifuged at 200 × g for 8 min to obtain pellets of 200,000 cells. Chondrogenic differentiation was induced by culturing the cells for 5 weeks in chondrogenic medium consisting of DMEM-high-glucose GlutaMAX+ (GIBCO), 1:100 insulin, transferrin, and selenous acid (ITS+; BD Biosciences), 40 μg ml^{-1} L-proline (Sigma-Aldrich), 1 mM sodium pyruvate (GIBCO), 100 nM dexamethasone (Sigma-Aldrich), 10 ng ml^{-1} transforming growth factor β1 (TGF-β1; R&D Systems), 1.5 μg ml^{-1} fungizone, and 50 μg ml^{-1} gentamicin. Medium was renewed twice a week. Alternatively, the WNT inhibitor IWP2 (2 μM) was added during the last 3 weeks of chondrogenic induction. For this experiment, medium was renewed three times per week.

Gene Expression Analysis

Cells in monolayers were washed with PBS and treated on ice with RLT lysis buffer (QIAGEN). After 3, 4, or 5 weeks in chondrogenic induction medium, pellets were manually homogenized in RNA-Bee (Tel-Test) and RNA was extracted by addition of 20% chloroform. In all cases, RNA was purified using an RNeasy Micro kit (QIAGEN) and 1 μg of total RNA was reverse transcribed into cDNA using a RevertAid First Strand cDNA synthesis kit (MBI Fermentas). Polymerase chain reactions were performed with TaqMan Universal PCR MasterMix (Applied Biosystems) or SYBR Green MasterMix (Fermentas) using an ABI PRISM 7000 apparatus. Primers and probe sets (Table S1) were designed using Primer Express 2.0 software (Applied Biosystems). Data were normalized to *GAPDH* after its identification as the more stable within the conditions and over time. Relative expression was calculated according to the $2^{-\Delta\Delta Ct}$ formula (Schmittgen and Livak, 2008).

Cartilage Stability In Vivo

Pellets from P2-expanded cells were implanted subcutaneously in 10- to 14-week-old female NMRI nu/nu mice (Charles River Laboratories). The mice were anesthetized using a mixture of isoflurane/O_2 and four pellets per donor and condition were implanted by a blinded technician in two separate subcutaneous pockets. After 8 weeks, the animals were sacrificed and the samples were harvested, fixed in 4% formalin, and subjected to a microcomputed tomography (μCT) scan. Afterward, samples were decalcified with 10% EDTA in PBS (pH 7.4) for 5 days and then paraffin embedded, sectioned, and used for (immuno)histochemistry. Animal experiments were carried out in the central animal facilities at Erasmus MC with approval of the Animal Experiments Committee according to the national animals act (EMC 2429).

(Immuno)Histochemistry

In Vitro Samples

Pellets were fixed in 4% formalin and paraffin embedded. Four sections (6 μm) of each sample were stained with 0.4% thionine solution (Sigma-Aldrich) in demineralized water to detect glycosaminoglycans or immunostained to detect collagen type II or collagen type X as previously described (Hellingman et al., 2010). Briefly, antigen retrieval was performed with 0.1% pronase (Sigma-Aldrich) in PBS for collagen type II and with 0.1% pepsin (Sigma-Aldrich) in 0.5 M acetic acid (pH 2.0) for collagen type X staining. Both stainings continued with incubation with 10 mg ml^{-1} hyaluronidase (Sigma-Aldrich) in PBS. Then, sections were incubated for 2 hr with primary antibody for collagen type II (II-II/II6B3; Developmental Studies Hybridoma Bank, University of Iowa) or 16 hr with collagen type X (2031501005; Quartett). Alkaline phosphatase-labeled secondary antibody was used in combination with Neu Fuchsine substrate, resulting in a red staining. An isotype IgG1

monoclonal antibody was used as a negative control. NIH ImageJ freeware was used to evaluate the size of the pellets on sections taken from the middle of the pellet and the percentage of the thionine-positive areas and to quantify the number of cells per mm^2 in the sections stained by thionine.

In Vivo Samples

After 8 weeks in vivo, pellets were decalcified as described above, paraffin embedded, sectioned, and either immunostained for collagen type II or stained with hematoxylin (Sigma-Aldrich) for 5 min followed by counterstaining with 2% eosin solution (Merck) in 50% ethanol. Collagen type II immunostaining was performed as described for the in vitro samples but using the primary antibody previously incubated overnight with a goat anti-mouse biotin-conjugated antibody (115-066-062; Jackson ImmunoResearch Europe). An isotype IgG1 monoclonal antibody was used as a negative control. All the (immuno)histological evaluations were performed in collaboration with an experimentally blinded technician.

DNA and Glycosaminoglycan Quantification

Pellets at days 3, 7, 10, 14, 17, 21, 24, 28, 31, and 35 of culture were digested with 300 μl of proteinase K solution (1 mg ml^{-1} proteinase K, 50 mM Trizma base, 1 mM EDTA, 1 mM iodoacetamide, 10 μg ml^{-1} pepstatin [pH 7.6]; all from Sigma-Aldrich) for 16 hr at 60°C. After digestion, proteinase K was inactivated for 10 min at 105°C.

DNA Quantification

Five to 20 μl of each proteinase K-digested sample was loaded in technical triplicate on an ice-cold 96-well plate. After incubation with heparin (8.3 U ml^{-1} in PBS; Leo Pharma) and RNase solution (0.05 mg ml^{-1} in PBS; Sigma-Aldrich), 50 μl of ethidium bromide (25 μg ml^{-1} in PBS; GIBCO) was added to each sample. Using the Wallac 1420 VICTOR^2 (PerkinElmer) apparatus, the ratio between the absorbance at 340 nm (extinction filter) and the absorbance at 590 nm (emission filter), corrected by the background (wells loaded with PBS only), was calculated. Purified calf thymus DNA (Sigma-Aldrich) was used to set the standard curve.

Glycosaminoglycan Assay

1,9-dimethylmethylene blue (DMB; Sigma-Aldrich) solution (46 μM DMB, 40 mM glycine, 40 mM NaCl [pH 3.0]) was added to proteinase K-digested samples (200 μl) and the 530:590 nm absorbance ratio was measured to determine the glycosaminoglycan amount, using chondroitin sulfate C (Sigma-Aldrich) as a standard.

MicroCT Analysis

After in vivo implantation, pellets from two MSC donors (n = 2 donors, four pellets per donor and condition) were analyzed by the Quantum FX μCT scanner (PerkinElmer) using the following settings: isotropic voxel size of 10 μm, 70 kV, 160 mA, 5 mm field of view, 3 min scan (FINE setting) per sample. Raw μCT images were converted into 3D reconstructions using Quantum FX μCT software (PerkinElmer).

Statistical Analysis

Data were analyzed with PASW Statistics 20 (SPSS). The normal distribution of data was confirmed using the Kolmogorov-Smirnov test. An unpaired t test or a generalized mixed model was applied; the different conditions were considered a fixed parameter and the donors as a random factor. In the case of multiple comparisons, Bonferroni post hoc test was performed. The extra sum of square F test was used to compare the polynomial regressions shown in Figures 2C and 3B. A Levene's test verified the equality of variances in the samples (homogeneity of variances). $p < 0.05$ was considered statistically significant.

SUPPLEMENTAL INFORMATION

Supplemental Information includes Supplemental Experimental Procedures, five figures, and two tables and can be found with this article online at http://dx.doi.org/10.1016/j.stemcr.2015.01.017.

AUTHOR CONTRIBUTIONS

R.N., D.t.B., and G.J.V.M.v.O. were responsible for study concept and design; R.N., M.A.C., N.T., and M.J.H. were responsible for the acquisition of data; R.N., D.t.B., M.A.C., P.A.J.B., and G.J.V.M.v.O. were involved in interpretation of data and preparation of the manuscript. All authors approved the final version of the manuscript.

ACKNOWLEDGMENTS

J. van der Stok, N. Kops, J. Lehmann, and J.L.M. Koevoet are acknowledged for technical assistance. This work was funded by the Netherlands Institute of Regenerative Medicine (grant FES0908) and Science Foundation Ireland (grant 11/RFP/BMT/3150). R.N. was further supported by Translational Adult Stem Cell Research by ZonMw (grant 116005009), and D.t.B. was further supported by TI Pharma (grant D5-402) and Marie Curie (grant FP7-PEOPLE-2009-RG-256560). R.N., M.A.C., and G.J.V.M.v.O. performed the research within the framework of the Erasmus Postgraduate School Molecular Medicine.

Received: August 11, 2014
Revised: January 21, 2015
Accepted: January 22, 2015
Published: February 26, 2015

REFERENCES

Auletta, J.J., Zale, E.A., Welter, J.F., and Solchaga, L.A. (2011). Fibroblast growth factor-2 enhances expansion of human bone marrow-derived mesenchymal stromal cells without diminishing their immunosuppressive potential. Stem Cells Int. *2011*, 235176.

Banfi, A., Muraglia, A., Dozin, B., Mastrogiacomo, M., Cancedda, R., and Quarto, R. (2000). Proliferation kinetics and differentiation potential of ex vivo expanded human bone marrow stromal cells: implications for their use in cell therapy. Exp. Hematol. *28*, 707–715.

Benya, P.D., Padilla, S.R., and Nimni, M.E. (1978). Independent regulation of collagen types by chondrocytes during the loss of differentiated function in culture. Cell *15*, 1313–1321.

Bianchi, G., Banfi, A., Mastrogiacomo, M., Notaro, R., Luzzatto, L., Cancedda, R., and Quarto, R. (2003). Ex vivo enrichment of

mesenchymal cell progenitors by fibroblast growth factor 2. Exp. Cell Res. *287*, 98–105.

Boland, G.M., Perkins, G., Hall, D.J., and Tuan, R.S. (2004). Wnt 3a promotes proliferation and suppresses osteogenic differentiation of adult human mesenchymal stem cells. J. Cell. Biochem. *93*, 1210–1230.

Bonab, M.M., Alimoghaddam, K., Talebian, F., Ghaffari, S.H., Ghavamzadeh, A., and Nikbin, B. (2006). Aging of mesenchymal stem cell in vitro. BMC Cell Biol. *7*, 14.

Brittberg, M., Lindahl, A., Nilsson, A., Ohlsson, C., Isaksson, O., and Peterson, L. (1994). Treatment of deep cartilage defects in the knee with autologous chondrocyte transplantation. N. Engl. J. Med. *331*, 889–895.

Cawthorn, W.P., Bree, A.J., Yao, Y., Du, B., Hemati, N., Martinez-Santibañez, G., and MacDougald, O.A. (2012). Wnt6, Wnt10a and Wnt10b inhibit adipogenesis and stimulate osteoblastogenesis through a β-catenin-dependent mechanism. Bone *50*, 477–489.

Chen, J., Sotome, S., Wang, J., Orii, H., Uemura, T., and Shinomiya, K. (2005). Correlation of in vivo bone formation capability and in vitro differentiation of human bone marrow stromal cells. J. Med. Dent. Sci. *52*, 27–34.

Cho, H.H., Kim, Y.J., Kim, S.J., Kim, J.H., Bae, Y.C., Ba, B., and Jung, J.S. (2006). Endogenous Wnt signaling promotes proliferation and suppresses osteogenic differentiation in human adipose derived stromal cells. Tissue Eng. *12*, 111–121.

Churchman, S.M., Ponchel, F., Boxall, S.A., Cuthbert, R., Kouroupis, D., Roshdy, T., Giannoudis, P.V., Emery, P., McGonagle, D., and Jones, E.A. (2012). Transcriptional profile of native CD271+ multipotential stromal cells: evidence for multiple fates, with prominent osteogenic and Wnt pathway signaling activity. Arthritis Rheum. *64*, 2632–2643.

Cooper, K.L., Hu, J.K., ten Berge, D., Fernandez-Teran, M., Ros, M.A., and Tabin, C.J. (2011). Initiation of proximal-distal patterning in the vertebrate limb by signals and growth. Science *332*, 1083–1086.

Day, T.F., and Yang, Y. (2008). Wnt and hedgehog signaling pathways in bone development. J. Bone Joint Surg. Am. *90* (*Suppl 1*), 19–24.

Day, T.F., Guo, X., Garrett-Beal, L., and Yang, Y. (2005). Wnt/beta-catenin signaling in mesenchymal progenitors controls osteoblast and chondrocyte differentiation during vertebrate skeletogenesis. Dev. Cell *8*, 739–750.

De Bari, C., Dell'Accio, F., and Luyten, F.P. (2004). Failure of in vitro-differentiated mesenchymal stem cells from the synovial membrane to form ectopic stable cartilage in vivo. Arthritis Rheum. *50*, 142–150.

Dennis, J.E., Merriam, A., Awadallah, A., Yoo, J.U., Johnstone, B., and Caplan, A.I. (1999). A quadripotential mesenchymal progenitor cell isolated from the marrow of an adult mouse. J. Bone Miner. Res. *14*, 700–709.

Dominici, M., Le Blanc, K., Mueller, I., Slaper-Cortenbach, I., Marini, F., Krause, D., Deans, R., Keating, A., Prockop, D.J., and Horwitz, E. (2006). Minimal criteria for defining multipotent mesenchymal stromal cells. The International Society for Cellular Therapy position statement. Cytotherapy *8*, 315–317.

Dong, Y.F., Soung, D.Y., Chang, Y., Enomoto-Iwamoto, M., Paris, M., O'Keefe, R.J., Schwarz, E.M., and Drissi, H. (2007). Transforming growth factor-beta and Wnt signals regulate chondrocyte differentiation through Twist1 in a stage-specific manner. Mol. Endocrinol. *21*, 2805–2820.

Etheridge, S.L., Spencer, G.J., Heath, D.J., and Genever, P.G. (2004). Expression profiling and functional analysis of Wnt signaling mechanisms in mesenchymal stem cells. Stem Cells *22*, 849–860.

Farrell, E., van der Jagt, O.P., Koevoet, W., Kops, N., van Manen, C.J., Hellingman, C.A., Jahr, H., O'Brien, F.J., Verhaar, J.A., Weinans, H., and van Osch, G.J. (2009). Chondrogenic priming of human bone marrow stromal cells: a better route to bone repair? Tissue Eng. Part C Methods *15*, 285–295.

Farrell, E., Both, S.K., Odörfer, K.I., Koevoet, W., Kops, N., O'Brien, F.J., Baatenburg de Jong, R.J., Verhaar, J.A., Cuijpers, V., Jansen, J., et al. (2011). In-vivo generation of bone via endochondral ossification by in-vitro chondrogenic priming of adult human and rat mesenchymal stem cells. BMC Musculoskelet. Disord. *12*, 31.

Gharibi, B., and Hughes, F.J. (2012). Effects of medium supplements on proliferation, differentiation potential, and in vitro expansion of mesenchymal stem cells. Stem Cells Transl. Med. *1*, 771–782.

Handorf, A.M., and Li, W.J. (2011). Fibroblast growth factor-2 primes human mesenchymal stem cells for enhanced chondrogenesis. PLoS ONE *6*, e22887.

Hellingman, C.A., Koevoet, W., Kops, N., Farrell, E., Jahr, H., Liu, W., Baatenburg de Jong, R.J., Frenz, D.A., and van Osch, G.J. (2010). Fibroblast growth factor receptors in in vitro and in vivo chondrogenesis: relating tissue engineering using adult mesenchymal stem cells to embryonic development. Tissue Eng. Part A *16*, 545–556.

Hellingman, C.A., Davidson, E.N., Koevoet, W., Vitters, E.L., van den Berg, W.B., van Osch, G.J., and van der Kraan, P.M. (2011). Smad signaling determines chondrogenic differentiation of bone-marrow-derived mesenchymal stem cells: inhibition of Smad1/5/8P prevents terminal differentiation and calcification. Tissue Eng. Part A *17*, 1157–1167.

Hermida-Gómez, T., Fuentes-Boquete, I., Gimeno-Longas, M.J., Muiños-López, E., Díaz-Prado, S., de Toro, F.J., and Blanco, F.J. (2011). Bone marrow cells immunomagnetically selected for CD271+ antigen promote in vitro the repair of articular cartilage defects. Tissue Eng. Part A *17*, 1169–1179.

Hsieh, J.C., Rattner, A., Smallwood, P.M., and Nathans, J. (1999). Biochemical characterization of Wnt-Frizzled interactions using a soluble, biologically active vertebrate Wnt protein. Proc. Natl. Acad. Sci. USA *96*, 3546–3551.

Im, G.I., and Quan, Z. (2010). The effects of Wnt inhibitors on the chondrogenesis of human mesenchymal stem cells. Tissue Eng. Part A *16*, 2405–2413.

Im, G.I., Lee, J.M., and Kim, H.J. (2011). Wnt inhibitors enhance chondrogenesis of human mesenchymal stem cells in a long-term pellet culture. Biotechnol. Lett. *33*, 1061–1068.

Isenmann, S., Arthur, A., Zannettino, A.C., Turner, J.L., Shi, S., Glackin, C.A., and Gronthos, S. (2009). TWIST family of basic helix-loop-helix transcription factors mediate human mesenchymal stem cell growth and commitment. Stem Cells *27*, 2457–2468.

Jullien, N., Maudinet, A., Leloutre, B., Ringe, J., Häupl, T., and Marie, P.J. (2012). Downregulation of ErbB3 by Wnt3a contributes to wnt-induced osteoblast differentiation in mesenchymal cells. J. Cell. Biochem. *113*, 2047–2056.

Li, Z., Liu, C., Xie, Z., Song, P., Zhao, R.C., Guo, L., Liu, Z., and Wu, Y. (2011). Epigenetic dysregulation in mesenchymal stem cell aging and spontaneous differentiation. PLoS ONE *6*, e20526.

Mankin, H.J. (1982). Alterations in the structure, chemistry, and metabolism of the articular cartilage in osteoarthritis of the human hip. Hip, 126–145.

Martin, I., Muraglia, A., Campanile, G., Cancedda, R., and Quarto, R. (1997). Fibroblast growth factor-2 supports ex vivo expansion and maintenance of osteogenic precursors from human bone marrow. Endocrinology *138*, 4456–4462.

Mastrogiacomo, M., Cancedda, R., and Quarto, R. (2001). Effect of different growth factors on the chondrogenic potential of human bone marrow stromal cells. Osteoarthritis Cartilage *9* (*Suppl 1*), S36–S40.

Mayne, R., Vail, M.S., Mayne, P.M., and Miller, E.J. (1976). Changes in type of collagen synthesized as clones of chick chondrocytes grow and eventually lose division capacity. Proc. Natl. Acad. Sci. USA *73*, 1674–1678.

McAlinden, A., Johnstone, B., Kollar, J., Kazmi, N., and Hering, T.M. (2008). Expression of two novel alternatively spliced COL2A1 isoforms during chondrocyte differentiation. Matrix Biol. *27*, 254–266.

Menicanin, D., Bartold, P.M., Zannettino, A.C., and Gronthos, S. (2010). Identification of a common gene expression signature associated with immature clonal mesenchymal cell populations derived from bone marrow and dental tissues. Stem Cells Dev. *19*, 1501–1510.

Muraglia, A., Cancedda, R., and Quarto, R. (2000). Clonal mesenchymal progenitors from human bone marrow differentiate in vitro according to a hierarchical model. J. Cell Sci. *113*, 1161–1166.

Pelttari, K., Winter, A., Steck, E., Goetzke, K., Hennig, T., Ochs, B.G., Aigner, T., and Richter, W. (2006). Premature induction of hypertrophy during in vitro chondrogenesis of human mesenchymal stem cells correlates with calcification and vascular invasion after ectopic transplantation in SCID mice. Arthritis Rheum. *54*, 3254–3266.

Pittenger, M.F., Mackay, A.M., Beck, S.C., Jaiswal, R.K., Douglas, R., Mosca, J.D., Moorman, M.A., Simonetti, D.W., Craig, S., and Marshak, D.R. (1999). Multilineage potential of adult human mesenchymal stem cells. Science *284*, 143–147.

Prockop, D.J. (1997). Marrow stromal cells as stem cells for nonhematopoietic tissues. Science *276*, 71–74.

Quarto, R., Mastrogiacomo, M., Cancedda, R., Kutepov, S.M., Mukhachev, V., Lavroukov, A., Kon, E., and Marcacci, M. (2001). Repair of large bone defects with the use of autologous bone marrow stromal cells. N. Engl. J. Med. *344*, 385–386.

Quarto, N., Behr, B., and Longaker, M.T. (2010a). Opposite spectrum of activity of canonical Wnt signaling in the osteogenic context of undifferentiated and differentiated mesenchymal cells: implications for tissue engineering. Tissue Eng. Part A *16*, 3185–3197.

Quarto, N., Wan, D.C., Kwan, M.D., Panetta, N.J., Li, S., and Longaker, M.T. (2010b). Origin matters: differences in embryonic tissue origin and Wnt signaling determine the osteogenic potential and healing capacity of frontal and parietal calvarial bones. J. Bone Miner. Res. *25*, 1680–1694.

Rabinowitz, A.H., and Vokes, S.A. (2012). Integration of the transcriptional networks regulating limb morphogenesis. Dev. Biol. *368*, 165–180.

Sacchetti, B., Funari, A., Michienzi, S., Di Cesare, S., Piersanti, S., Saggio, I., Tagliafico, E., Ferrari, S., Robey, P.G., Riminucci, M., and Bianco, P. (2007). Self-renewing osteoprogenitors in bone marrow sinusoids can organize a hematopoietic microenvironment. Cell *131*, 324–336.

Schmittgen, T.D., and Livak, K.J. (2008). Analyzing real-time PCR data by the comparative C(T) method. Nat. Protoc. *3*, 1101–1108.

Scotti, C., Tonnarelli, B., Papadimitropoulos, A., Scherberich, A., Schaeren, S., Schauerte, A., Lopez-Rios, J., Zeller, R., Barbero, A., and Martin, I. (2010). Recapitulation of endochondral bone formation using human adult mesenchymal stem cells as a paradigm for developmental engineering. Proc. Natl. Acad. Sci. USA *107*, 7251–7256.

Solchaga, L.A., Penick, K., Porter, J.D., Goldberg, V.M., Caplan, A.I., and Welter, J.F. (2005). FGF-2 enhances the mitotic and chondrogenic potentials of human adult bone marrow-derived mesenchymal stem cells. J. Cell. Physiol. *203*, 398–409.

Solchaga, L.A., Penick, K., Goldberg, V.M., Caplan, A.I., and Welter, J.F. (2010). Fibroblast growth factor-2 enhances proliferation and delays loss of chondrogenic potential in human adult bone-marrow-derived mesenchymal stem cells. Tissue Eng. Part A *16*, 1009–1019.

ten Berge, D., Brugmann, S.A., Helms, J.A., and Nusse, R. (2008a). Wnt and FGF signals interact to coordinate growth with cell fate specification during limb development. Development *135*, 3247–3257.

ten Berge, D., Koole, W., Fuerer, C., Fish, M., Eroglu, E., and Nusse, R. (2008b). Wnt signaling mediates self-organization and axis formation in embryoid bodies. Cell Stem Cell *3*, 508–518.

ten Berge, D., Kurek, D., Blauwkamp, T., Koole, W., Maas, A., Eroglu, E., Siu, R.K., and Nusse, R. (2011). Embryonic stem cells require Wnt proteins to prevent differentiation to epiblast stem cells. Nat. Cell Biol. *13*, 1070–1075.

Tsutsumi, S., Shimazu, A., Miyazaki, K., Pan, H., Koike, C., Yoshida, E., Takagishi, K., and Kato, Y. (2001). Retention of multilineage differentiation potential of mesenchymal cells during proliferation in response to FGF. Biochem. Biophys. Res. Commun. *288*, 413–419.

Venkatesan, J.K., Ekici, M., Madry, H., Schmitt, G., Kohn, D., and Cucchiarini, M. (2012). SOX9 gene transfer via safe, stable,

replication-defective recombinant adeno-associated virus vectors as a novel, powerful tool to enhance the chondrogenic potential of human mesenchymal stem cells. Stem Cell Res. Ther. *3*, 22.

Willert, K., Brown, J.D., Danenberg, E., Duncan, A.W., Weissman, I.L., Reya, T., Yates, J.R., III, and Nusse, R. (2003). Wnt proteins are lipid-modified and can act as stem cell growth factors. Nature *423*, 448–452.

Yang, D.C., Yang, M.H., Tsai, C.C., Huang, T.F., Chen, Y.H., and Hung, S.C. (2011). Hypoxia inhibits osteogenesis in human mesenchymal stem cells through direct regulation of RUNX2 by TWIST. PLoS ONE *6*, e23965.

Zeller, R., López-Ríos, J., and Zuniga, A. (2009). Vertebrate limb bud development: moving towards integrative analysis of organogenesis. Nat. Rev. Genet. *10*, 845–858.